Protein Partitioning in Two-Phase Aqueous Polymer Systems. 1. Novel Physical Pictures and a Scaling-Thermodynamic Formulation

Nicholas L. Abbott, Daniel Blankschtein,* and T. Alan Hatton

Department of Chemical Engineering, Massachusetts Institute of Technology, Cambridge, Massachusetts 02139

Received November 1, 1990; Revised Manuscript Received March 4, 1991

ABSTRACT: Novel physical pictures are proposed for the interactions between globular proteins and flexible nonionic polymers that are responsible for the observed partitioning of proteins in two-phase aqueous polymer systems. For the system poly(ethylene oxide) (PEO)–dextran–water these novel physical pictures are based on the observation that a transition occurs in the nature of the top PEO-rich phase, from the dilute to the semidilute polymer solution regimes, with increasing PEO molecular weight. In systems containing low molecular weight PEO ($M < 10\,000$ Da), *individual polymer coils*, which may be larger or smaller than the proteins, interact with the proteins. Mathematically simple geometric and scaling arguments are used to probe the qualitative form of the free-energy change arising from polymer–protein and polymer–polymer interactions within each picture. Through a statistical thermodynamic framework, used to relate the change in free energy to the experimentally measurable protein partition coefficient, K_p, it is possible to discriminate between the novel physical pictures on the basis of the predicted qualitative trends. At Θ-solvent conditions for the polymer, a picture that incorporates solely the excluded-volume interactions between the proteins and the polymer coils is unable to account for the influence of polymer molecular weight on K_p; at athermal-solvent conditions, where repulsive polymer–polymer interactions also influence the protein chemical potential, the predicted protein partition coefficient is shifted in a direction qualitatively consistent with experimental trends. For both athermal- and Θ-solvent conditions, the observed change in K_p is found to be qualitatively consistent with the presence of a weak attraction between the polymer coils and the proteins. The presence of a strong attraction between the polymer coils and the proteins, and associated formation of an adsorbed polymer layer at the surface of the proteins, can lead to a new partitioning behavior that has not yet been realized experimentally. In systems containing high molecular weight PEO ($M \gg 10\,000$ Da), the proteins interact with an *entangled polymer network* rather than with identifiable polymer coils, and the protein partition coefficient becomes independent of the PEO molecular weight.

1. Introduction

The physics controlling the interactions between globular colloidal particles and flexible chain macromolecules is reflected in such diverse phenomena as the complexation of polymers and micelles;[1-8] the polymeric stabilization and flocculation of gold sols,[9] ceramic particles,[10] and other colloidal dispersions;[11] and the stabilization, aggregation, and precipitation of proteins.[12-15] In the case of the adsorption of hydrophilic polymers onto the surfaces of ionic micelles in aqueous solutions, experimental measurements[1-8] have revealed a variety of interesting physical pictures for these systems. For example, in dilute aqueous polymer solutions, anionic micelles adsorb onto a polymer coil giving rise to structures resembling beads on a necklace.[5] In addition, theory, particularly in the form of scaling arguments, has complemented the experimental measurements and revealed important differences in the nature of polymer adsorption onto small globular colloids as compared to planar surfaces having infinite areas.[16-18]

A class of systems that bears a remarkable similarity to the complex micelle–polymer fluids, but that has remained relatively unexplored at the molecular level, is aqueous solutions of flexible polymers and globular proteins. These systems are particularly interesting under conditions where the polymer solution undergoes phase separation.[19,20] In the resulting two-phase aqueous polymer system, proteins usually distribute unevenly between the two coexisting polymer solution phases. This unequal distribution reflects an intricate and delicate balance of interactions between the protein and polymer species in each of the coexisting polymer solution phases.

To a large extent, interest in the partitioning behavior of proteins and other biomolecules in two-phase aqueous polymer systems has been stimulated by the potential of these polymer solutions to provide immiscible, yet protein compatible, liquid phases for the purification of proteins by liquid–liquid extraction.[19-22] This has been triggered by recent advances in the development of new techniques to produce proteins on a large scale and the need to devise novel separation principles on comparable scales. Liquid–liquid extraction using two-phase aqueous polymer systems appears a promising approach. Since each of the two coexisting phases contains predominantly water, proteins may be dissolved in these systems while maintaining their native conformation and biological activity. In fact, the presence of polymers may even enhance protein stability against thermal denaturation.[19]

In general, the distribution of proteins between the two aqueous polymer solution phases is characterized by a partition coefficient, K_p, defined as

$$K_p = c_{p,t}/c_{p,b} \tag{1}$$

where $c_{p,t}$ and $c_{p,b}$ are the protein concentrations in the top (t) and bottom (b) polymer solution phases, respectively. Experimental measurements of protein partition coefficients have revealed that the properties of the proteins, for example, the size, conformation, and composition, appear important in determining the protein distribution between the two phases.[23-25] In addition, the type of phase-forming polymers,[19] their molecular weight[24,26] and concentration,[27-29] and the presence of any chemical moieties attached to the polymer (ligands) that

* Author to whom correspondence should be addressed.

0024-9297/91/2224-4334$02.50/0

may interact specifically with surface sites on proteins,[30-35] constitute important factors. Furthermore, the addition of salts to these systems appears to create a Donnan-type electrical potential difference between the two coexisting phases and can therefore influence the partitioning of the charged protein species.[19,20] Since the net charge on the protein depends on the pH of the solution, changes in solution pH can dramatically affect protein partitioning.[21,36,37] In addition, changes in protein partition coefficients with pH may also reflect an alteration of the hydrated layer surrounding the protein, which mediates the interaction of the phase-forming polymers and the protein. High salt concentrations can also affect the protein distribution between the phases by changing the polymer compositions of the coexisting phases and thus affecting the interactions between proteins, polymers, and solvent in a very complex manner that also appears related to the polar nature of water.[38]

Despite the existence of an extensive literature reporting experimental investigations of protein partitioning phenomena in two-phase aqueous polymer systems, a plethora of important and fundamental questions regarding the nature of the interactions responsible for the observed phenomena remain unanswered.[39] Indeed, relatively scant attention has been devoted to the development of a molecular level understanding of the interactions between flexible phase-forming polymers and globular proteins and the extent to which these interactions influence the partitioning behavior.

It is not within the scope of this paper to provide a detailed review of prior modeling approaches of protein partitioning in two-phase aqueous polymer systems. A more complete discussion may be found in a number of recent publications.[39,40] For brevity, we will simply emphasize how our approach goes beyond those previous approaches that are most relevant to the present theoretical developments.

In the present paper, we pursue a molecular description of the interactions of proteins and nonionic polymers with an emphasis on the development of physical pictures of these complex solutions. In particular, in contrast to Brooks et al.[41] and Albertsson et al.[24] who utilized the Flory–Huggins lattice model[42,43] for polymer solutions to describe protein partitioning, and thus treated the protein as a third flexible and random coiling polymer component, we have represented the relatively rigid and structured globular protein as a compact colloid. Furthermore, we go beyond the physical description explored by Baskir et al.[27,44] who have extended a self-consistent mean-field model[45,46] for the adsorption of flexible polymers onto planar surfaces to the case of a spherical geometry associated with the protein. For example, the latter approach neglects fluctuations and correlations between polymer segments in the system, where the range can be larger or smaller than the protein size for the two-phase aqueous polymer systems considered in their work; that is, it assumes the polymer solution to be extensively interpenetrating over all molecular weights of the polymers and neglects correlations between polymer segments within the interpenetrating polymer network. In contrast, we recognize here that the polymer solutions of low molecular weight polymers contain identifiable and singly dispersed polymer coils, and we have explored the influence of such a scenario on the partitioning of proteins. Indeed, this region is of great interest since it is in this range of polymer molecular weights that the partition coefficient of the protein is most sensitive to the polymer molecular weight, as we show later. Finally, our approach contrasts with the virial expansion approaches of King et al.[29] and Forciniti and Hall.[47] King et al.[29] *measured* the interaction parameters of the virial expansion using low-angle laser light scattering in the mixtures containing the protein, water, salts, and one of the polymer types and, to date, the interpretation of the interaction parameters in terms of molecular mechanisms has not yet been reported. Although Forciniti and Hall[47] explored the role of excluded-volume interactions on protein partitioning, at the protein isoelectric point, by calculating the virial interaction parameters, they did not consider the influence of the transition in the nature of the polymer solution phases with polymer molecular weight, which is revealed in the present paper.

Within a statistical thermodynamic framework that relates the change in the free energy of interaction between polymers and proteins to the protein partition coefficient, we have utilized simple geometric and scaling arguments[48] to capture the essential features of the interactions between polymers and proteins for each different physical picture proposed, as well as to obtain the various forms of the free energy of interaction. The essence of the scaling arguments is to capture the universal features characterizing the polymer–protein interactions. As such, the lack of cumbersome and complex computations permits us to concentrate on the underlying physical content of the formulation. For the systems we are considering, this approximate physical description is consistent with our model of globular protein molecules as rigid and impenetrable spheres with homogeneous surface properties. Although simple, our treatment of the protein molecules appears justified by the strong correlation between the protein partition behavior and geometric protein properties such as hydrodynamic size, as will be described in section 2 and is illustrated in Figure 2. To date, with few exceptions, scaling descriptions of the interactions of polymers and small rigid colloids have treated systems in which a single polymer chain dominates the interactions with each colloid.[16,17] For the partitioning of proteins in two-phase aqueous polymer systems we demonstrate that this is not always the limit of interest. Consequently, we have generalized some earlier scaling descriptions to include the possibility of multiple polymer interactions with each colloid.

The remainder of the paper is organized as follows. Section 2 presents some brief comments on a compilation of experimental results that are central to the theoretical developments described in this paper. Section 3 discusses a thermodynamic formulation to relate the protein partition coefficient to the free-energy change arising from the interactions of protein and polymer species. In section 4, the varying physical nature of the polymer solution phases is identified, and the appropriate length scales to describe the interactions between protein and polymer are identified. In section 5, the development of physical pictures of the polymer solution phases containing proteins is detailed, scaling relations for the free energy of interaction of the protein and polymers for each picture are proposed, and, where possible, the predictions are compared with experiments. Finally, section 6 presents our conclusions and comments on future research directions.

2. Experimental Observations

The measured partition coefficients, K_p, of a variety of globular proteins reported by Hustedt et al.[26] and Albertsson et al.[24] are presented in Figure 1 for the two-phase aqueous polymer system containing the polymers poly(ethylene oxide) (PEO) and dextran. In this system, the top phase is rich in PEO and the bottom phase is rich in dextran. The response of the protein partition coefficients to changes in the molecular weight of PEO indicates the

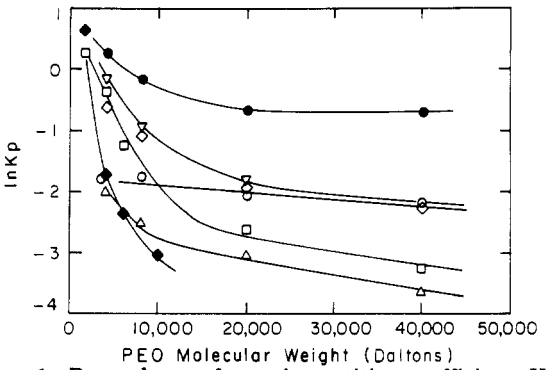

Figure 1. Dependence of protein partition coefficient, K_p, on PEO molecular weight in a PEO–dextran–water system: (○) cytochrome *c*; (●) ovalbumin; (◇) bovine serum albumin; (△) lactate dehydrogenase; (▽) catalase; (□) pullulanase; (◆) phosphorylase. Data compiled from Hustedt et al.[26] and Albertsson et al.[24]

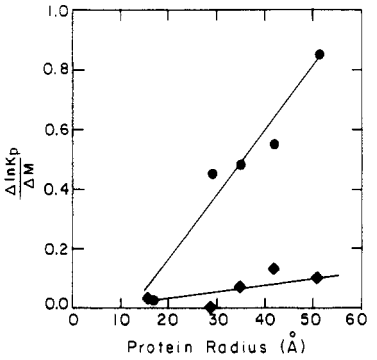

Figure 2. Change in protein partition coefficient (per 4000 Da PEO), $\Delta \ln K_p/\Delta M$, with PEO molecular weight for five proteins, (●) 4000–8000 Da; (◆) 20 000–40 000 Da. The data are taken from Figure 1. In order of increasing size the proteins are cytochrome *c*, ovalbumin, bovine serum albumin, lactate dehydrogenase, and catalase.

following three features for these proteins in this system: (1) An increase in the molecular weight of PEO results in the partition of the proteins away from the top PEO-rich phase, and hence in a decrease in ln K_p, (2) the protein response to the change in PEO molecular weight is greatest at PEO molecular weights below approximately 10 000 Da as reflected by the rapid decrease in ln K_p over this molecular weight range, and (3) the response of the proteins to changes in PEO molecular weight is protein specific. Feature (3) is further reflected in Figure 2, where the change in the protein partition coefficient (per 4000 Da PEO), $\Delta \ln K_p/\Delta M$, measured when the PEO molecular weight is varied from 4000 to 8000 Da (as shown by the circles) or from 20 000 to 40 000 Da (as shown by the diamonds), is given as a function of the hydrodynamic radii of the proteins. For example, in the region of low PEO molecular weight ($M < 10\,000$ Da), a doubling of the PEO molecular weight from 4000 to 8000 Da caused a change in the logarithm of the partition coefficient for ovalbumin (with a radius of 29 Å) of 0.44 kT per 4000 Da of PEO. In contrast, for two-phase systems containing high molecular weight poly(ethylene oxide) ($M > 10\,000$ Da), a change in the PEO molecular weight from 20 000 to 40 000 Da caused negligible change in the logarithm of the partition coefficient (per 4000-Da change in PEO molecular weight). For all the proteins shown in Figure 2 it is apparent that this behavior is a general feature with the difference in partitioning between the low and high PEO molecular weight regions increasing with protein size.

For the systems in which the protein partition coefficients were measured by Albertsson et al.,[24] the weight fractions of each of the phase-forming polymers in both the upper and lower phases are shown in Figure 3. The

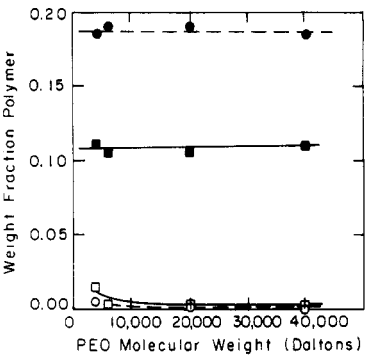

Figure 3. Weight fraction of PEO and dextran in the top and bottom phases as a function of PEO molecular weight; (●) dextran in bottom phase; (○) dextran in top phase; (■) PEO in top phase; (□) PEO in bottom phase. Data compiled from ref 19.

constancy of the phase compositions over the range of PEO molecular weights investigated by Albertsson et al.[24] suggests, to a first approximation, that the origin of trends measured in the protein partition coefficients with protein size and polymer molecular weight are not founded in variations of the phase compositions which may, in general, accompany changes in PEO molecular weight. Note that the insensitivity of the phase compositions (% w/w) to the polymer molecular weight is due to the fact that the composition of the system is far from the critical point composition. Furthermore, it is evident from Figure 3 that each phase contains essentially only one type of polymer species. Typically, the concentration of the minor polymer species is less than 1% w/w.

3. Thermodynamic Formulation

A thermodynamic formulation is required to relate the free energy changes associated with the interactions between proteins and polymers to the experimentally accessible protein partition coefficient. Experimental measurements performed in the limit of vanishing protein concentration, namely, high protein dilutions, simplify the connection between the required free-energy changes and the protein partition coefficient, as it can be assumed that the proteins do not interact with each other significantly during measurement of the protein partition coefficient and thus may be assumed to be isolated from each other. As expected, in this limit, the protein partition coefficient is generally observed to become independent of protein concentration.[19] Note that although the experimental conditions reduce the influence of protein–protein interactions on the partition coefficient, we recognize that proteins can associate under certain conditions, particularly near their isoelectric point.[49] Furthermore, the presence of polymers may promote the association or dissociation of proteins, depending on the polymer type and protein species.[15] Therefore, although the independence of the protein partition coefficient on protein concentration provides some justification for the assumed minor role of protein–protein interactions on protein partitioning, this topic warrants further investigation, particularly for those proteins that are known to self-associate. Another useful simplification that arises from the measurement of K_p at high protein dilution is that these low protein concentrations cause a negligible perturbation to the two-phase equilibrium of the phase-forming polymers in the absence of the proteins. A typical protein concentration is 1 g/L (<0.1 mM) and thus the latter assumption appears reasonable and has been confirmed by experiments.[50] Finally, we consider each phase to contain water, protein, and only one of the two polymers present in the system. Provided that the two-

phase systems are far from their critical points, the concentration of the minority polymer is very low as is apparent from Figure 3, and hence this assumption appears very reasonable.

In general, the protein chemical potential in phase i (t or b) is given by

$$\mu_{p,i} = \mu^\circ_{p,i} + kT \ln (c_{p,i}\gamma_{p,i}) + z_{p,i}(\psi_i - \psi_o) \quad (2)$$

where $\mu^\circ_{p,i}$ is the standard-state chemical potential of the protein in phase i, k is the Boltzmann factor, T is the absolute temperature, $\gamma_{p,i}$ is the activity coefficient of the protein at concentration $c_{p,i}$, $z_{p,i}$ is the net protein charge in phase i, and ψ_i and ψ_o are the electrical potentials of phase i and a reference phase o, respectively. Note that the last term in eq 2 arises from the necessary presence of buffering salts in the system to control pH. The equilibrium distribution of proteins between two coexisting phases is determined by the equality of the chemical potentials in each phase, that is, by $\mu_{p,t} = \mu_{p,b}$. Furthermore, in the absence of significant protein–protein interactions (see discussions above), the protein activity coefficient in each phase is approximately unity. Using this information and eq 2, the protein partition coefficient is given by

$$\ln K_p = \ln\left(\frac{c_{p,t}}{c_{p,b}}\right) = \left(\frac{\mu^\circ_{p,b} - \mu^\circ_{p,t}}{kT}\right) + \left(\frac{z_p(\psi_b - \psi_t)}{kT}\right) \quad (3)$$

where the net charge of the protein has been assumed to be independent of the phase in which the protein resides, that is, $z_{p,t} = z_{p,b} = z_p$. This assumption is supported by the small pH difference between the two coexisting phases, as well as by the almost uniform partition of most salts between the phases.[19] In general, experimental investigations have revealed that $\psi_b - \psi_t$ can be influenced by the specific salt types in the system and the concentrations of the polymers in each of the coexisting phases.[19,29] Since only very small changes are measured in the phase polymer compositions (% wt/wt) over the PEO molecular weight range of interest (see Figure 3), to a reasonable approximation, by examining changes in the protein partition coefficient with PEO molecular weight for a given salt (buffer) type and concentration, eq 3 suggests that one probes only those factors that affect the standard-state chemical potentials of the proteins. Note that an assumption implicit in the prior statement is that $\psi_b - \psi_t$ is not significantly influenced by the PEO molecular weight. This can be justified, in part, if one considers the interactions between salts and PEO to be short-ranged, that is, if salt interacts with PEO at the length scale of the polymer segments rather than the polymer coil size. Indeed, the precise nature of the interactions of nonionic polymers and salts remains to be elucidated, although some experimental evidence (see below) supports our assertion. Under the above assumptions, the change in the protein partition coefficient accompanying changes in the PEO molecular weight reduces to

$$\Delta \ln K_p = \Delta \ln\left(\frac{c_{p,t}}{c_{p,b}}\right) = \left(\frac{\mu^\circ_{p,b,2} - \mu^\circ_{p,b,1}}{kT}\right) - \left(\frac{\mu^\circ_{p,t,2} - \mu^\circ_{p,t,1}}{kT}\right) \quad (4)$$

Note that the symbol $\Delta \ln K_p$ denotes the change in the protein partition coefficient between two systems containing different PEO molecular weights, defined as states 1 and 2. We now return briefly to the assumptions leading to the cancellation of the electrical potential term in eq 4. If this is justified, the change in the protein partition coefficient predicted by eq 4, $\Delta \ln K_p$, should be independent of the salt type present in the system, which is indeed observed experimentally.[51] In addition, since a very low concentration of PEO is present in the bottom dextran-rich phase, we assume that only the protein standard-state chemical potential term in the top PEO-rich phase changes with changes in PEO molecular weight. This further simplifies eq 4, yielding

$$\Delta \ln K_p = -\left(\frac{\mu^\circ_{p,t,2} - \mu^\circ_{p,t,1}}{kT}\right) \quad (5)$$

Equation 5 is a central result which indicates that, under the assumptions detailed above, changes in the protein partition coefficient are essentially determined by the interactions of the protein in the top PEO-rich solution phase. Note that, in the present case, the physical meaning of the protein standard-state chemical potential is the excess free energy change upon introducing a single isolated protein from a polymer-free solvent into a polymer solution phase. Indeed, the standard-state protein chemical potential is an excess free-energy because the contribution arising from the ideal entropy of mixing the protein with the polymer solution is contained in the logarithmic term of eq 2 (with $\gamma_{p,i} = 1$). In evaluating this free energy change we have made an additional simplifying assumption regarding the proteins. That is, we have treated the proteins as rigid impenetrable spheres with homogeneous surface properties and have assumed that all properties of the protein may be uniformly averaged over the entire molecule. As previously mentioned, this simple view of the proteins is justified by the clear correlation between the protein partition coefficient and the characteristic protein size (see Figures 1 and 2), which suggests that other factors, for example, amino acid composition and distribution throughout the protein, may be less important than the protein size in determining the interactions with flexible polymers. It should be kept in mind, however, that proteins generally have rather inhomogeneous surface properties and possess structures that can fluctuate about a mean conformation. The incorporation of these additional protein properties into the description of protein–polymer interactions is likely to be necessary for any detailed quantitative treatment of these interactions.

4. Development of Physical Pictures

In this paper we focus our attention on the interactions of globular proteins and PEO as some useful experimental measurements exist in the literature that reflect these interactions.[24,26,29] To elucidate the character of the interactions between polymers and proteins, an appreciation of the physical nature of the polymer solution is required. In particular, the characteristic length scale of the polymer solution needed to describe the interactions between the polymers and the protein must be identified.

In the two-phase aqueous polymer systems of interest, the molecular weights of the PEO molecules are typically low, for example, Albertsson et al.[24] used PEO molecular weights of 4000 Da and above. We therefore examine the nature of PEO in a structured solvent such as water and consider the applicability of polymer concepts to such species. PEO in the crystalline state possesses a helical structure.[52] Upon dissolution in water, Raman,[53,54] infrared,[55] and nuclear magnetic resonance spectroscopies,[55,56] as well as ultrasonic attenuation measurements,[57] suggest the retention, to some extent, of the helical ordering present in crystalline PEO. Alternatively, investigations of high molecular weight PEO in water using viscosity,[58–60] small-angle neutron scattering (SANS), and light scattering measurements[5] reveal typical polymer-like behavior. For example, the exponent relating the polymer radius of

gyration, R_g, to the molecular weight, M, is 0.62 and independent of the molecular weight for high molecular weight PEO,[5] as predicted by Flory[42] and polymer scaling arguments.[48] Therefore, one can conclude that high molecular weight PEO in water behaves as a quasi-random coil having some solvent-induced short-range order along the backbone of the polymer.[60] For low molecular weight PEO the evidence is less conclusive. There is an absence of appropriate SANS and light scattering data below PEO molecular weights of 10 000 Da, and the issue of partial coil drainage prevents the interpretation of viscosity data for low molecular weight polymers in terms of the polymer configuration.[59,61] However, the elution of PEO in the molecular weight range of 1000–6000 Da in water using size-exclusion chromatography was found to be only slightly affected by the addition of 6 M guanidine.[62] As 6 M guanidine disrupts hydrogen bonding in aqueous solution, this suggests that hydrogen bonding in aqueous solutions of low molecular weight PEO, at least, does not control the configuration of the polymer coils significantly. This observation, along with the flexibility of high molecular weight PEO, suggests that it is reasonable to treat PEO of molecular weight down to, at least, 4000 Da with conventional polymer concepts.

To elucidate the nature of the aqueous PEO solution comprising the top PEO-rich phase, we found it instructive to examine the PEO crossover concentration, c^*, as a function of PEO molecular weight, which can be estimated from

$$c^* = \frac{M}{\frac{4\pi}{3}R_g^3} \tag{6}$$

where M and R_g are the molecular weight and radius of gyration of the PEO polymer molecules, respectively.[48] Equation 6 defines the characteristic concentration of polymer mass within each polymer coil volume. Clearly, when the actual concentration of polymer in the solution exceeds this characteristic concentration, the coils are overlapping. In other words, the crossover concentration, c^*, is a polymer concentration characteristic of the region where the extensive overlap of polymer coils begins to occur. At polymer concentrations, c, much less than c^* the solution is dilute in polymer coils and consequently the identity of each individual polymer coil is preserved, and the solution properties reflect the identities of the individual polymer coils. In contrast, when the polymer concentration is much greater than c^*, the polymer coils, no longer separated by regions of solvent, overlap and entangle with each other to form a continuous polymer web or net. Within this web, the identities of the individual polymer coils are lost, and all thermodynamic properties of the solution become independent of the molecular weight of the polymer coils. For aqueous solutions of PEO, the values of c^*, calculated from eq 6 as a function of polymer molecular weight, M, are reported as the full line in Figure 4. Also shown in Figure 4 is the measured PEO concentration in the top PEO-rich phase (data points with dashed line) for the systems in which the protein partition coefficients were measured by Albertsson et al.[19,24] The two curves intersect in the vicinity of a PEO molecular weight of 10 000 Da, indicating that in going from a low to a high PEO molecular weight, the nature of the top PEO-rich solution phase undergoes a profound change. This is an important observation, as it suggests that the change in the measured protein partition coefficients with increasing PEO molecular weight may, in fact, reflect the changing nature of the polymer solution in the top PEO-rich phase. This also suggests that the interactions of proteins and polymers will be quite different in the limits of low and high PEO molecular weights. Important objectives of this paper are to characterize the changing nature of these interactions between proteins and polymers and to investigate how these changes relate to the trends observed in the experimentally measured protein partition coefficients.

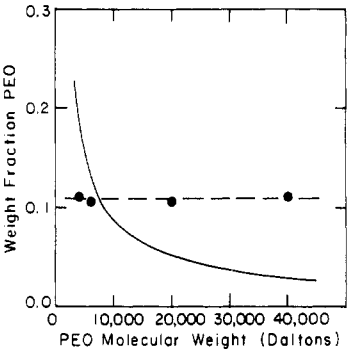

Figure 4. Polymer concentration, c^*, characterizing the transition from dilute to semidilute polymer solution regimes, evaluated from eq 6 as a function of PEO molecular weight (full line) and the measured PEO concentration, c, in the top PEO-rich phase (●).

5. Interactions of Proteins and Low Molecular Weight Polymers

We consider polymer solution phases rich in PEO having molecular weights of less than approximately 10 000 Da as low molecular weight polymer solutions. In these solutions, for which $c < c^*$, the identities of the individual polymer molecules are preserved, and the important characteristic length scale to consider is the polymer coil size, described by its radius of gyration, R_g. For the range of PEO molecular weights typically encountered in protein partitioning experiments, the polymer coil radius of gyration and the protein hydrodynamic radius have comparable sizes. Note, however, that the polymer can be larger or smaller than the protein, depending on the specific protein species and particular PEO molecular weight. Although in section 4 we have established that individual polymer coils will be present in PEO solution phases of low PEO molecular weight, the underlying physical nature of the polymer solution in the presence of proteins also depends, in part, on the relative strength of the interactions between the polymer coils and the globular protein molecules.

The novel physical pictures proposed in this paper for the interactions of globular proteins and flexible polymers are inspired, in part, by the analogy that we envision between the interactions of proteins and polymers and the interactions of ionic micelles and polymers. Indeed, ionic micelles and proteins can have similar shapes and sizes, and to some extent both micelles and proteins have charged surfaces and hydrophobic interiors. This analogy appears fruitful because the interactions of ionic micelles and polymers have been the subject of a number of experimental investigations.[1-8] In particular, the structure of the aqueous polymer–micelle system containing PEO and sodium dodecyl sulfate (SDS) anionic micelles has been studied in some detail by a variety of techniques including dialysis,[2] conductivity,[1] surface tension,[63] dye solubilization,[1] nuclear magnetic resonance,[4] and small-angle neutron scattering.[5,6] A conclusion supported by these experiments is the existence of a strong attraction between the anionic micelles and the PEO coils. More generally, it appears that interactions between polymers

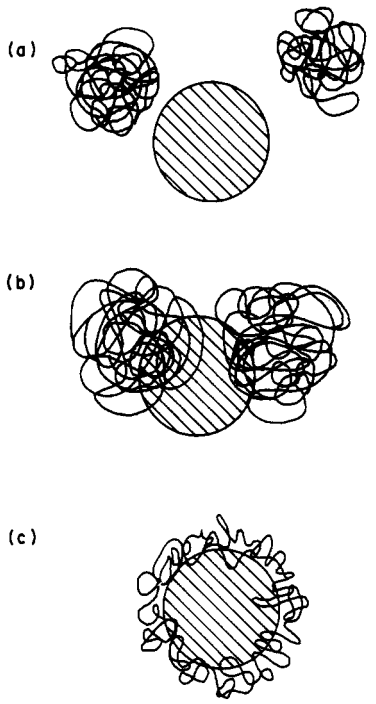

Figure 5. Three pictures representing the possible nature of the interactions between proteins and low molecular weight polymers: (a) picture 1, only physical exclusion exists; (b) picture 2, a weak attraction exists between the polymer and the protein in addition to physical exclusion; (c) picture 3, a stronger attraction between the polymer coils and the protein causes the formation of an adsorbed polymer layer about the protein. For details, see section 5.

and micelles depend on the extent to which the polymer shields the micellar hydrocarbon cores from water, as well as on the magnitude of steric and electrostatic interactions (e.g., between charges and dipoles) between the polar surfactant head groups and the polymer segments.[64] For example, the interaction of PEO with cationic micelles is found to be weaker than that with anionic micelles,[64] and negligible interactions of PEO with nonionic micelles have been reported.[4] Therefore, by analogy, interactions of both the protein charges and the more hydrophobic amino acid residues with PEO may provide an attraction between the protein and the polymer segments. In proposing possible physical pictures of polymer–protein solutions, we have included the possible existence of such attractive interactions.

Although the similarities of ionic micelles and proteins have been emphasized and will be exploited in our theoretical formulation, we recognize that other properties of these two colloids differ from each other. For example, the structures of globular proteins are often stabilized by the formation of intramolecular covalent disulfide bonds, which impart a degree of rigidity to the protein. In contrast, the assembly of surfactant molecules into a micellar structure is driven by purely physical forces and results in a less rigid assembly than a protein and allows the continual exchange of surfactant molecules between micelles as well as surfactant monomers in solution.

Since the specific nature of the interactions between proteins and polymers appears unknown, we have explored a variety of possible physical pictures, which differ primarily in the strength of the polymer coil interaction with the protein. Three pictures representing the nature of the interactions of proteins and low molecular weight PEO molecules are presented in Figure 5. The first picture, Figure 5a, presents a scenario where the only interaction between the protein and the polymer coils is a physical excluded-volume interaction. That is, the free-energy change resulting from the introduction of a protein into the PEO solution arises solely as a consequence of the change in the number of configurations available to the system. The second picture, Figure 5b, describes a scenario where a very weak attraction exists between the protein and polymer coils in addition to the excluded volume interaction. Specifically, the attractive interaction is not strong enough to cause the collapse of the polymer coils onto the protein surface. Consequently, the polymer coils remain essentially undeformed in the vicinity of the protein surface. If the attractive interaction between the protein and the polymer coils increases in strength, the polymer coil will deform and actually adsorb onto the protein surface thus forming a polymer–protein complex. This third scenario is reflected in Figure 5c. The deformation of the polymer from its relaxed configuration in the bulk solution, characterized by R_g, to a pancake-shaped configuration, characterized by thickness $D \ll R_g$, concentrates the polymer segments in the vicinity of the protein surface and thus increases the number of contacts between each polymer coil and the protein surface. Limiting the extent of polymer adsorption is the loss of polymer conformations, as well as an increase in the excluded-volume interactions between the polymer segments present in the adsorbed layer.

5.1. Picture 1. The first picture, Figure 5a, assumes that the sole contribution to the free-energy change associated with introducing a protein into an aqueous PEO solution arises from the change in the number of configurations available to the system, in other words, a change in the entropy of the system. The precise meaning of the entropy of mixing in the present case is the entropy change resulting from mixing a single protein molecule, polymers, and solvent relative to mixing polymers and solvent in the absence of the protein. Note that prior to mixing the protein with polymer and solvent, the protein is considered to be in a solvent phase, and therefore the protein is assumed not to change its state, for example, hydration characteristics and average configurational state, when mixed with the polymer and the solvent.

At constant temperature and volume, and therefore assuming negligible volume change upon mixing the protein and the polymers, the standard-state chemical potential of the protein is equal to the change in the Helmholtz free energy[65] of the system per protein introduced into the system, that is

$$\mu^\circ_{p,t,i} = \delta A^\circ_{p,t,i} \tag{7}$$

where $\delta A^\circ_{p,t,i}$ is the Helmholtz free-energy change upon introducing a single and isolated protein molecule into the top (t) PEO-rich solution phase at conditions i ($i = 1$ or 2). For a change in the PEO molecular weight (denoted by the symbol Δ), and using eq 5, we find that

$$\Delta \ln K_p = -\left(\frac{\delta A^\circ_{p,t,2} - \delta A^\circ_{p,t,1}}{kT}\right) \tag{8}$$

In picture 1, no change in internal energy accompanies the transfer of a protein into the polymer solution phase, and consequently the Helmholtz free-energy change can be directly related to the change in the entropy,[65] that is, $\delta A^\circ_{p,t,i} = -T\delta S^\circ_{p,t,i}$. With this in mind, eq 8 becomes

$$\Delta \ln K_p = \left(\frac{\delta S^\circ_{p,t,2} - \delta S^\circ_{p,t,1}}{k}\right) \tag{9}$$

The isothermal entropy of mixing the protein with the polymer solution is related to the number of configurations adopted by the various components of the solution through

$$\frac{\delta S^{\circ}_{p,t,i}}{k} = \ln \Omega_{N_p=1}(N_2,V,T) - \ln \Omega_{N_p=0}(N_2,V,T) \quad (10)$$

where $\Omega_{N_p=1}$ and $\Omega_{N_p=0}$ are the numbers of polymer solution configurations with and without the protein present, respectively, and N_2 is the number of polymer molecules in the system volume V.

Assuming that the number of ways of placing a polymer molecule in the volume V is proportional to the available free volume with a proportionality constant A_2 (see Appendix 1), the number of configurations $\Omega_{N_p=0}$ is given by[49]

$$\Omega_{N_p=0} = \frac{A_2^{N_2}(V-U_1)(V-U_2)...(V-U_{N_2})}{N_2!} \quad (11)$$

where U_j is the volume excluded by the $j-1$ polymer coils present in the system. Thus, $V - U_j$ is the free volume available to the jth polymer coil as it is placed sequentially in the volume V. For example, $U_1 = 0$, since the entire system volume V is available for the placement of the first polymer coil. The factor $N_2!$ accounts for the indistinguishability of the polymer coils. The major difficulty in the evaluation of eq 11 is the assignment of excluded volumes U_j.[49,66] In the dilute polymer solution regime we assume that the excluded volumes are additive; that is, $U_j = (j-1)U_2$, where U_2 is the volume excluded by each polymer coil in the system. In that case, expanding the various natural logarithms appearing in $\ln \Omega_{N_p=0}$ in terms of the expansion parameters $(j-1)U_2/V \ll 1$ to quadratic order yields

$$\ln \Omega_{N_p=0} = \ln (A_2^{N_2}) - \ln (N_2!) + N_2 \ln V - \frac{U_2 N_2^2}{2V} - \frac{U_2^2 N_2^3}{6V^2} \quad (12)$$

where the result $N_2(N_2-1) \simeq N_2^2$ for $N_2 \gg 1$ has been used.

We have extended the above approach to estimate the number of configurations of the polymer solution in which a protein molecule is dissolved. In general, the protein has a different size than each polymer coil. In the evaluation of the number of configurations, we place the N_p proteins (where $N_p = 1$) in the volume V first and follow it by the successive placement of the N_2 polymer coils. The logarithm of the number of configurations available to the solution, $\ln \Omega_{N_p=1}$, is obtained by expanding the various natural logarithms in terms of the expansion parameters $U_2(j-1)/(V-U_pN_p) \ll 1$. To quadratic order this yields

$$\ln \Omega_{N_p} = \ln (A_2^{N_2}A_p^{N_p}) - \ln (N_2!) + N_2 \ln (V - N_pU_p) + N_p \ln V - \ln (N_p!) - \frac{U_pN_p(N_p-1)}{2V} - \frac{U_2N_2^2}{2(V-N_pU_p)} - \frac{U_2^2N_2^3}{6(V-U_pN_p)^2} \quad (13)$$

where U_p is the volume excluded by the protein to the polymer coils and A_p is the proportionality constant relating the fraction of the system volume accessible to the protein (free volume) to the possible configurations of the system when the protein is introduced. Note that for $N_p = 0$, that is, with no protein present, eq 13 correctly reduces to eq 12. Setting $N_p = 1$ in eq 13, corresponding to a single protein in the system, followed by the substitution of eqs 12 and 13 into eq 10, yields

$$\frac{\delta S^{\circ}_{p,t,i}}{k} = \ln (A_pV) + N_2 \ln \left(1 - \frac{U_p}{V}\right) - \frac{U_2N_2^2(U_p/V)}{2V\left(1-\frac{U_p}{V}\right)} - \frac{U_2^2N_2^3(U_p/V)\left(1-\frac{1}{2}\frac{U_p}{V}\right)}{3V^2\left(1-\frac{U_p}{V}\right)^2} \quad (14)$$

In eq 14 the term $\ln (A_pV)$, which depends on the magnitude of the system volume, V, describes the ideal mixing of the protein in a volume V. As this term is also accounted for in the second term of the protein chemical potential in eq 2, and therefore does not contribute to the standard-state chemical potential of the protein as defined in that equation, we subtract it from eq 14. In the dilute protein solution limit of interest to us, for which $U_p \ll V$, we can further expand eq 14 to leading order in U_p/V. Carrying out this expansion and substituting the resulting expression in eq 9 yield

$$\Delta \ln K_p = -\Delta\left(\frac{N_2U_p}{V}\left(1 + \frac{N_2U_2}{2V} + O\left(\frac{N_2U_2}{V}\right)^2\right)\right) \quad (15)$$

Clearly, the truncation present in eq 15 produces an insignificant error provided that

$$\left(\frac{N_2U_2}{V}\right)^2 \ll 1 \quad (16)$$

From eq 16 it is apparent that the validity of the truncation depends upon both the number density of polymer coils in the solution, N_2/V, and the strength of the polymer–polymer interactions, characterized by U_2, which depends upon the solvent conditions. Therefore, we consider two typical types of solvent conditions corresponding to the so-called athermal- and Θ-solvent conditions for the polymer.[48] Athermal-solvent conditions prevail when there is no enthalpy change upon mixing polymer and solvent from the pure component states. In the absence of an enthalpy change upon mixing, the interactions between polymer coils are strongly repulsive due to excluded-volume interactions. In the notation of Flory[42] and Huggins,[43] this condition is characterized by $\chi = 0$, where χ is the Flory–Huggins interaction parameter. The Θ-solvent condition corresponds to the presence of an effective attraction between polymer coils that exactly balances the repulsive excluded-volume interactions and is characterized by $\chi = 0.5$. PEO in water at ambient conditions lies between these two limits with a Flory–Huggins interaction parameter, χ, of typically 0.45.[67,68] Consequently, by examining these two limits we hope to bound the behavior of the PEO–water (and salt) system.

In picture 1, the polymer–protein interaction is characterized by U_p. For globular proteins, which are relatively rigid (as compared to flexible random coiling polymers) and effectively impenetrable to the polymer, the assignment of the characteristic dimension of the protein needed to describe the exclusion of the polymer corresponds closely to the hydrodynamic radius of the protein. Furthermore, owing to the presence of relatively strong intramolecular forces within the protein it is unlikely that weak intermolecular interactions, for example, those with nonionic polymers, will cause large deformations of the protein structure. Indeed, the maintenance of enzymatic activity in most aqueous nonionic polymer solutions suggests, at the very least, the absence of changes in the protein structure associated with the active sites of the proteins.[19,20] Contrasting this situation is the behavior of flexible and deformable polymers, where the average configuration of an *isolated* molecule reflects a delicate balance of the in-

tramolecular forces. Furthermore, at finite concentrations, intermolecular interactions will also influence the polymer coil configurations. That is, in polymer solutions of finite concentration, polymer coil configurations will reflect both intra- and intermolecular interactions, effectively coupling these two factors. Note also that the average configurations of the flexible polymer coils associated with polymer–polymer interactions may differ from those associated with polymer–protein interactions as a result of the differing nature of the intermolecular interactions in the two cases. Specifically, for the interactions of globular proteins and flexible polymer coils, the characteristic dimension of the polymer coils for the description of the polymer–protein interaction will differ, in general, from that used to describe the polymer–polymer interactions. In particular, the former characteristic dimension will depend upon the relative sizes of protein and polymer. This fact is evident in an evaluation[69-71] of the excluded volume between polymers (at the Θ-solvent condition) and impenetrable spheres, over a size range that includes polymers that are either smaller or larger than the impenetrable sphere size. The excluded volume, U_p, was evaluated by the analogy between the flight of a diffusing particle and the statistics of ideal polymer coils (that is, polymer coils that possess no excluded volume and hence correspond to Θ-solvent conditions) and is given by[71]

$$U_p = 4\pi R_p R_g^2 + 8\pi^{1/2} R_p^2 R_g + \frac{4\pi R_p^3}{3} \tag{17}$$

Note that the qualitative form of eq 17 is different in the limits $R_g \ll R_p$ (the protein and polymer interact at their surfaces since the protein is too large to penetrate to any significant extent into the polymer coil volume) and $R_g \gg R_p$ (a significant number of polymer coil configurations exist which permit the protein to diffuse unhindered into the volume occupied, on average, by the polymer coil). Note that, for the proteins reported in Figure 1 and for PEO in the molecular weight range from 4000 to 10 000 Da, the size ratio of interest occurs in the interval $0.4 < R_g/R_p < 2.5$.

Case 1: Θ-Solvent. At Θ-solvent conditions for the polymer, the enthalpy of interaction between the polymer coils and solvent exactly balances the excluded-volume interactions between polymer coils, implying that $U_2 = 0$. Therefore, eq 16 is always satisfied. Using the fact that $U_2 = 0$ in eq 15 yields

$$\Delta \ln K_p = -\Delta\left(\frac{N_2 U_p}{V}\right) \tag{18}$$

When comparing the prediction of $\Delta \ln K_p$ to the experimentally observed trends in the protein partition coefficient, it is important to note that the change in the polymer molecular weight occurs at constant weight fraction of the polymer in the solution. This fact was emphasized in Section 2. Therefore, accompanying a change in the polymer molecular weight is not only a change in the polymer coil size but also changes in both the number concentration of polymer coils and the associated volume of the solution excluded by polymer coils. At constant weight fraction of polymer in the solution, the number of polymer coils per unit volume, N_2/V, scales with the number of polymer segments per polymer coil, N, as $1/(NV)$. However, since the volume of the system, V, is constant, for simplicity we omit the term V hereafter and use the scaling relation

$$N_2/V \sim 1/N \tag{19}$$

For a polymer coil at Θ-solvent conditions, the radius of gyration scales as[42,48]

$$R_g \sim aN^{1/2} \tag{20}$$

where a is the characteristic size of a polymer segment. If eqs 17, 19, and 20 are substituted into eq 18, the protein partition coefficient is predicted to have the form

$$\Delta \ln K_p \sim -\Delta\left(4\pi R_p a^2 + 8\pi^{1/2} R_p^2 a N^{-1/2} + \frac{4\pi R_p^3 N^{-1}}{3}\right) \tag{21}$$

With the exponent of N constrained to negative values, the qualitative behavior of the experimentally determined protein partition coefficients shown in Figure 1 cannot be reproduced. Such a behavior requires that this exponent be greater than 0. To understand the behavior predicted by eq 21 we return to eq 18, which reflects two clear contributions. The first one arises from the term N_2/V, the number concentration of polymer coils in the solution, which is a measure of the frequency of interaction between the protein and the polymer coils. The second one, U_p, the volume excluded by the protein from the polymer coils, is a measure of the strength of the polymer–protein excluded-volume interaction. It is the competition between these two factors that leads to the predicted behavior. An increase in the polymer molecular weight (recall that N is proportional to polymer molecular weight), at constant weight fraction of polymer in the solution, results both in a decreased frequency of interaction (since N_2/V decreases, see eq 19) as well as in an increase in the strength of the excluded-volume interaction (since U_p increases, see eqs 17 and 20). For Θ-solvent conditions the former factor dominates for small polymers, whereas for large polymers the two factors balance each other.

Case 2: Athermal Solvent. For a polymer in an athermal solvent, the repulsive excluded-volume interactions between polymer coils causes U_2 to be greater than zero. Therefore, the validity of the truncation presented in eq 15 is not guaranteed and the condition in eq 16 must be satisfied to justify the truncation. Clearly, if eq 16 is satisfied, this constraint dictates that the second term in eq 15, which contains the influence of the polymer–polymer steric interactions (through U_2) on $\ln K_p$, cannot dominate the first term. Recall that the first term describes the contribution of the direct protein–polymer interaction to the protein chemical potential. In other words, because eq 16 must be satisfied to justify the truncation present in eq 15, it is not possible, in the context of the formalism developed so far, to predict protein partitioning behavior under conditions where polymer–polymer steric interactions dominate the form of the protein chemical potential. Nevertheless, it is of interest to examine the direction of the influence of polymer–polymer interactions on the partition coefficient of the protein (under conditions where eq 16 is satisfied) in addition to the influence of the athermal-solvent conditions on the direct protein–polymer interaction. This will be done in the spirit of a scaling approach. For polymer coils in athermal solvents, the excluded volume describing the interactions between equal sized polymer coils can be described by the polymer coil radius of gyration[49] as

$$U_2 \sim a^3 N^{9/5} \tag{22}$$

where we have used the fact that $R_g \sim aN^{3/5}$ for a polymer coil in an athermal solvent.[42,48] Note that U_2 is proportional to the spherical volume defined by R_g. To determine the form of the excluded volume that characterizes the interaction between the polymer coil in an athermal solvent and the protein we have adopted eq 17 suggested by Janson and Phillips.[71] Although eq 17 was derived for a

Θ-solvent, we utilize it for polymer coils in an athermal solvent, using the appropriate scaling relation (shown above) to connect the polymer radius of gyration to the number of polymer segments per polymer coil. This approach for describing the qualitative features of polymer–protein interactions in an athermal solvent is supported by a Monte Carlo calculation of U_p.[72] By substitution of eq 17 (with $R_g \sim aN^{3/5}$ and U_2 given in eq 22) and eq 19 into eq 15 and with numerical prefactors neglected, the following expression for $\Delta \ln K_p$ results

$$\Delta \ln K_p \sim -\Delta\left(\left(4\pi R_p a^2 N^{1/5} + \frac{8\pi^{1/2} R_p^{\,2} a}{N^{2/5}} + \frac{4\pi R_p^{\,3}}{3N}\right) \times (1 + pa^3 N^{4/5})\right) \quad (23)$$

where p is an order of unity numerical prefactor. Recall from the discussion above that the term $(1 + pa^3N^{4/5})$ in eq 23 describes the influence of polymer–polymer interactions on the protein chemical potential and thus on the protein partition coefficient. The essence of the result in eq 23 may be summarized as

$$\Delta \ln K_p \sim -\Delta(R_p^{\alpha} N^{\beta} N^{\gamma}) \quad (24)$$

where the exponents are constrained to lie in the limits $1 < \alpha < 3$, $-1 < \beta < {}^1/_5$, and $0 < \gamma < {}^4/_5$. In eq 24, the exponents α and β describe the influence of the protein size and polymer molecular weight, respectively, on $\Delta \ln K_p$ through direct polymer–protein interactions, whereas γ captures the influence of the polymer molecular weight on $\Delta \ln K_p$ through polymer–polymer interactions. As noted earlier, the exponent of N must be greater than 0 to describe the experimental trends. Although this appears unlikely to result from β, as β decreases to -1 with decreasing N, it is important to note that the influence of the polymer–polymer interaction (through γ) is in the direction of the experimental trends in the protein partition coefficient. Indeed, the possibility that a more quantitative and detailed treatment of the entropy of mixing of protein and polymers may account entirely for the protein partition coefficient cannot be discarded. From this analysis it is evident that important features to be incorporated in future developments include the deformability and permeability of the polymer coils in the presence of the globular proteins, the partial permeability of the polymer coils to each other (which varies with the solvent condition), and the contributions of higher order interactions between polymer coils and proteins. Work in this direction is in progress.

5.2. Picture 2. In the second picture, Figure 5b, a weak attractive interaction between the polymer coils and the protein molecules is introduced to determine the influence of such weak attractions on the protein partition coefficient. Owing to the assumed weakness of the attraction we have treated it as a perturbation of the repulsive excluded-volume interactions considered in section 5.1. Although in this paper we have assumed the range of the attractive forces to be small relative to the size of the protein and polymer coils, we are aware that forces such as those of the van der Waals type can be significant between dense colloidal spheres and polymers and can act over length scales comparable to the typical dimensions of the protein and the polymer coils. Therefore, a more detailed treatment may consider the interactions of the entire protein molecule with the polymer coils, rather than the surface-type interactions of range a, the polymer segment size, characterized by an energy ϵ, considered below. Defined more precisely, ϵ is the local energy change (measured in units of kT) that accompanies the replacement of solvent at the protein surface by one polymer segment. Provided that ϵ is sufficiently weak, the presence of the attraction will not significantly influence the frequency of contacts between a polymer coil and a globular protein (as compared to the random mixing case). This is in contrast to the third picture to be treated in section 5.3, where an increase in ϵ beyond a certain threshold value results in the extensive deformation of the polymer coil and the associated formation of an adsorbed polymer layer about the protein.

The contribution of the attraction between the polymer coils and the protein to the standard-state protein chemical potential, $\mu_p^{o,att}$, in the polymer solution can be considered to have the following form

$$\frac{\mu_p^{o,att}}{kT} \sim -\left(\frac{N_2 V_c}{V}\right)\langle m_s\rangle \epsilon \quad (25)$$

Equation 25 results from a consideration of binary interactions between the protein and the polymer coils. Note that although the contribution of the attraction between protein and polymer to the free energy of the solution is proportional to both the protein concentration, N_p/V, and polymer concentration, N_2/V, the protein chemical potential is only linear in N_2/V. The combined term $(N_2/V)V_c$ reflects the fact that in a dilute polymer solution the likelihood of contact between the polymer coils and the protein increases with both the polymer coil concentration, N_2/V, and the sizes of the protein and polymer coils, both of which are reflected in the term V_c. More specifically, with the center of mass of the protein fixed in space, V_c, is the total volume traced out by the center of mass of the polymer coil for which the polymer coil has an attractive interaction energy $\langle m_s\rangle\epsilon$ with the protein. The term $\langle m_s\rangle$ is the characteristic number of contacts between a polymer coil and a protein, averaged over all polymer configurations for which at least one contact has occurred between the polymer coil and the protein. In the above formulation, the qualitative forms of V_c and $\langle m_s\rangle$ depend upon the relative sizes of the protein and the polymer. We consider first a situation where the polymer coil size is either smaller than or similar to that of the protein, that is, $R_g \leq R_p$, and subsequently show that our general treatment is also physically reasonable in the limit $R_g \gg R_p$.

In the limit $R_g \leq R_p$, on average, very few configurations of the polymer chain permit the protein to penetrate the polymer–coil volume, which is characterized by R_g^3. For the case of interest here, where the range of the attractive interactions is of order a, V_c scales as $(R_g + R_p)^2 a$, the volume of a shell having an area of order $(R_g + R_p)^2$ and a thickness of order a. The term $\langle m_s\rangle$ is estimated as

$$\langle m_s\rangle \sim \rho^* A_c a \quad (26)$$

where ρ^* is the characteristic polymer segment density at the protein surface and A_c is the area of contact between the protein and the polymer coil, which depends, in general, on the sizes and deformability of both species. Since the attractive interaction is weak, the deformation of the polymer coil due to the attraction is considered to be small in the vicinity of the protein (in contrast to picture 3), and thus the density of polymer segments at the protein surface will scale with the density of polymer segments within a polymer coil far from the protein surface. In particular, for athermal-solvent conditions (Θ-solvent conditions will

be considered later)

$$\rho^* \sim \frac{N}{\frac{4\pi}{3}R_g^3} \sim \frac{N}{(aN^{3/5})^3} \sim \frac{1}{a^3N^{4/5}} \quad (27)$$

When the protein and the polymer coil are similar in size, the curvature of the protein surface will reduce the available contact area for the polymer below that corresponding to an infinite planar surface. To account for this, we have estimated the contact area between the protein and the polymer coil, A_c, as R_{eff}^2, where R_{eff} is an effective radius between the protein and the polymer coil defined as

$$\frac{1}{R_{eff}} \sim \frac{1}{R_p} + \frac{1}{R_g} \quad (28)$$

Although other forms for the effective radius can be proposed, eq 28 is a conveniently simple representation, which also tends to a physically reasonable limit for $R_g \ll R_p$. In this latter limit, the number of contacts between the polymer coil and the protein is limited by the size of the polymer coil and naturally is independent of the protein dimension.

Using the above result for A_c in eq 25, along with eqs 26–28, the scaling form for the contribution of the attraction to the standard-state protein chemical potential for athermal-solvent conditions is given by

$$\mu_p^{o,att}/kT \sim -(N_2/V)\epsilon R_p^2 aN^{2/5} \quad (29)$$

Although our treatment of picture 2 includes a number of simplifications, the essence of the approach is supported by evaluations of $\langle m_s \rangle$ using Monte Carlo techniques to generate the configurations of a self-avoiding chain in the vicinity of a hard sphere for $R_g \leq R_p$, the region of behavior accessible to the simulation.[73] In particular, the scaling prediction that the contribution of the attraction to the protein standard-state chemical potential becomes more favorable with increasing polymer molecular weight (at constant N_2/V) for $R_g \leq R_p$ was verified, as was the predicted influence of the protein size on $\langle m_s \rangle$.

From eqs 5, 19, and 29, the contribution of the attractive interaction to the protein partition coefficient (for athermal-solvent conditions) is given by

$$\Delta \ln K_p^{att} \sim \Delta\left(\frac{\epsilon a R_p^2}{N^{3/5}}\right) \quad (30)$$

For Θ-solvent conditions, eqs 25–28 lead to the same scaling form for $\Delta \ln K_p^{att}$ with the exception that the exponent of N in eq 30 changes from $^3/_5$ to $^1/_2$. Note that the contribution of the entropy of mixing (excluded-volume interactions) to the protein partition coefficient, for both athermal solvents and Θ-solvents, is the same as that derived for picture 1 (see eq 15). In other words, eq 30 represents the contribution of the attraction between protein and polymers to the change in the protein partition coefficient and not the total change in the protein partition coefficient.

Equation 30 predicts two qualitative features of the protein partition coefficient, both of which are consistent with trends observed in experimental measurements of K_p (see Figures 1 and 2). First, with increasing polymer molecular weight, or equivalently with increasing N, the protein partition coefficient is predicted to decrease, in a manner consistent with Figure 1, and, second, the magnitude of this decrease in the protein partition coefficient is predicted to increase with protein size. This is also observed experimentally as shown in Figure 2. While allowance for a weak attraction between protein and polymer coils gives results that are consistent with experimental observations, this is not the case when the attraction is significantly stronger; as shown in section 5.3, the presence of a stronger attraction produces a strikingly different behavior due to the formation of an adsorbed layer of polymer about the protein. For a hard sphere of radius b, Pincus et al.[17] estimated the sticking energy necessary to form an adsorbed polymer layer around the sphere to be of order a/b (in units of kT), where a is the polymer segment size and translational entropy effects associated with forming the adsorbed layer are neglected. This estimate corresponds to an ϵ value of order 0.1 (in units of kT) for typical protein and polymer segment dimensions encountered in protein partitioning in two-phase aqueous polymer systems, and this may be considered to represent a bound between pictures 2 and 3. In section 5.3, we explore this latter scenario and show that formation of an adsorbed polymer layer about the protein is qualitatively inconsistent with the measured protein partition coefficients presented in Figure 1. Finally, it is important to note that, although the presence of a weak attraction between the polymer coils and the protein exerts an influence on the protein partition coefficient that is consistent with experimental measurements, without the precise numerical prefactor in eq 30 it is not possible to predict the relative magnitude of this contribution and that arising from the entropy of mixing (see eq 15) to the protein partition coefficient.

It is also of interest to briefly consider the influence of the weak attraction between the polymer coils and the protein in the alternative limit of $R_g \gg R_p$. In this limit, the polymer coil becomes penetrable to the protein and thus both V_c and $\langle m_s \rangle$ exhibit a different behavior from that corresponding to the previous case $R_g \leq R_p$. The difference between the behaviors of V_c and $\langle m_s \rangle$ in the limits $R_g \gg R_p$ and $R_g \leq R_p$ arises because of the difference in the ability of the protein to penetrate the polymer coil volume. As discussed above, in the limit $R_g \leq R_p$, the protein is sufficiently large (in comparison to the polymer coil) so as to sample the average properties of the polymer coil. On the other hand, when $R_g \gg R_p$, the protein is so small as to only sample local domains within the polymer coil, the properties of which are independent of the overall polymer coil configuration. Therefore, in the limit $R_g \gg R_p$, V_c becomes linear in N, corresponding to a long cylindrical shell of thickness a that encases the contour of the linear polymer chain, and consequently $\langle m_s \rangle$ becomes independent of N. These observations combined with eq 25 predict that the contribution of the attraction to the protein chemical potential, in the limit of high polymer molecular weight, will be independent of the polymer molecular weight (at constant weight fraction of polymer). For this latter limit it is interesting to compare and contrast our approach to the treatment due to Alexander,[16] who has proposed scaling descriptions for the free energy of interaction between an impenetrable sphere and a single polymer coil in the presence of a weak attractive interaction. Note that Alexander[16] was considering the limit of $N \to \infty$, where the entropy of mixing the sphere and polymer vanishes, and the sphere is located within the polymer coil with a probability approaching unity. The form proposed[16] for the change in the free energy of the system upon introducing the sphere into the polymer system was

$$\frac{F_{att}}{kT} \sim -\frac{\epsilon R_p^2}{a^2N^{4/5}} \quad (31)$$

for the polymer coil in an athermal solvent. Note that a direct and simple comparison of eqs 30 and 31 cannot be

made as eq 31 is derived for a single polymer coil in solution. Consequently, in eq 31, accompanying an increase in polymer coil molecular weight there must also be an increase in polymer weight fraction. In contrast, the polymer weight fraction remains constant in eq 30. Accordingly, it should be realized that the approaches leading to eqs 30 and 31 differ in the following ways. First, we have included a probability, $(N_2/V)V_c$, that the protein resides in the vicinity of the polymer coil and have also accounted for the entropy contribution to the protein chemical potential arising from the mixing of polymers and protein (as described in picture 1). Second, and perhaps more importantly, Alexander[16] considers a scenario where the small spheres within the polymer coil experience the average density of segments within the coil, ρ^*. In other words, the spheres experience an average attractive field, associated with the average segment concentration, that decreases with N. In contrast, we consider spheres that are sufficiently small to penetrate the polymer coil volume and experience a local interaction with polymer segments, which is independent of N, rather than sample the average properties of the entire polymer coil. It is important to note that this latter conclusion regarding the influence of the attractive interaction as N increases is consistent with the predicted independence of the excluded-volume interaction on N observed in the same limit (see section 5.1). This is reasonable, since in this limit both the excluded-volume interactions and the attractions reflect the interactions of the protein with local polymer segments rather than with the entire polymer coil.

Although we have determined that the presence of a weak attraction is consistent with experimental observations, which is similar to the conclusion reached by Baskir et al.,[27,44] it is important to appreciate the difference in the underlying physics treated in picture 2 as compared to that incorporated by Baskir et al.[27,44] In particular, they did not treat the low molecular weight polymer solutions as dilute and thus neglected the correlations between polymer segments that arise because they belong to identifiable polymer coils in the polymer solution phases. Instead, the polymer segment concentration was smeared uniformly over the bulk solution volume and the polymer solution interaction with the protein was described in terms of a continuum of polymer segments rather than discrete polymer coils. In contrast, we suggest that the trends observed in the protein partition coefficient (see Figure 1) can be a consequence of the existence of identifiable polymer coils in the solutions of low molecular weight polymer. In picture 2, it is precisely this changing nature of the polymer solution and the associated change in the extent of solution inhomogeneity on the length scale of the protein that cause the attraction between the protein and the polymer to influence the protein partition coefficient in a manner consistent with trends observed experimentally. In such inhomogeneous polymer solutions, the protein is able to experience an environment that does not correspond to the macroscopic volume average, as assumed in the model of Baskir et al.[27,44] It is interesting to note that the presence of the very weak attraction between PEO coils and the proteins is consistent with observations of a very weak adsorption of proteins onto hydrogel surfaces.[74]

5.3. Picture 3. In this third scenario, as shown in Figure 5c, the attractive interactions of the polymer segments and the protein are sufficiently strong to cause the collapse of the polymer coil into a pancake shape, with an associated spreading along the protein surface to form an adsorbed polymer layer. The adsorbed layer of polymer coils on the protein surface is characterized by a length scale D, the characteristic thickness of the adsorbed layer, and by m, the number or fraction of polymer coils contained within the adsorbed layer. Depending on the relative size of the polymer coil and the protein, more than one polymer may participate in the formation of the adsorbed layer ($m > 1$), one polymer may dominate the interaction with the protein ($m \sim 1$), or, in the limit of the polymer size being much larger than that of the protein, only a fraction of the polymer molecule may saturate the surface of the protein ($m \ll 1$). Previously, Alexander[16] and Pincus et al.[17] proposed scaling relations for the interactions of colloidal spheres with one polymer, and their work has provided the foundations for the generalized scaling analysis proposed for picture 3.

We consider the free-energy expression describing the interactions of the polymers and the proteins to contain five physically distinguishable contributions. The first three contributions, shown in eq 32, are simple extensions of results derived by Alexander[16] and Pincus et al.,[17] and therefore only the results and essential comments will be given. The reader is referred to the earlier papers[16,17] for further details. These first three terms scale as

$$\frac{F_{123}}{kT} \sim -Nm\epsilon f + k_1 m\left(\frac{R_g}{D}\right)^2 + \frac{k_2(mN)^2\nu}{2((R_p + D)^3 - R_p^3)} \quad (32)$$

where f is the fraction of polymer segments in the adsorbed layer of thickness D at the protein surface, k_1 and k_2 are order unity numerical prefactors, and ν is the polymer segment excluded-volume parameter. Briefly, the first term in eq 32 arises from the formation of favorable contacts between the polymer segments and the protein where the fraction f has the following scaling form:[17]

$$f \sim \frac{3k_3R_p^2a}{(R_p + D)^3 - R_p^3} \quad (33)$$

In eq 33, the constant k_3 is an order unity numerical prefactor. The second term in eq 32 accounts for the loss of configurational freedom accompanying the deformation of the polymer from a relaxed and unperturbed random-coil conformation far from the protein (characterized by R_g) to a pancake-shaped configuration in the adsorbed layer (characterized by D). Finally, accompanying the formation of the adsorbed polymer layer about the protein, there is an increase in the extent of the repulsive excluded-volume interaction between the polymer segments, which is captured in the third term of eq 32. To evaluate this contribution we have used a simple scaling form based on a mean-field approximation for the interactions between polymer segments, as well as a description of the adsorbed polymer layer as a local entangled mesh of polymer solution.[48] The form of this contribution to the free energy, F_3, is obtained by evaluating the work required to concentrate the polymer segments in the adsorbed layer against an osmotic pressure due to the excluded-volume interactions between the polymer segments. In an entangled mesh of polymer, the osmotic pressure is dominated by pairwise interactions between polymer segments and thus scales as c^2, where c is the concentration of polymer segments within the adsorbed layer of thickness D and is characterized by a term of the form $mN/((R_p + D)^3 - R_p^3)$.[16,17] Note that the denominator of the third term in eq 32 is the volume of the adsorbed polymer layer, that is, the volume over which the osmotic pressure is integrated to obtain the free energy. A reference term describing the extent of these same types of interactions between polymer segments within unperturbed polymer

coils in the bulk polymer solution is[42,48]

$$\frac{F_4}{kT} = -\frac{9(6^{1/2})k_4\nu m N^{1/5}}{2\pi} \quad (34)$$

where k_4 is an order unity numerical prefactor. Note that the sum of the third term in eq 32 and eq 34 describes the change in the extent of polymer segment interactions in going from the unperturbed polymer coil state to the state characterizing the adsorbed polymer layer on the protein surface.

The final important contribution to the free energy of interaction arises from a change in the translational entropy of the system that accompanies the complexation of m polymer molecules with each protein and the subsequent mixing of the complex with the remaining $N_2 - m$ free polymer coils in the polymer solution. The derivation of this term, F_5, which is presented in the Appendix, is analogous to the development of the entropy of mixing in section 5.1. The resulting expression is

$$\frac{F_5}{kT} = -m \ln\left(\frac{N_2 V_1^\circ}{V}\right) + \frac{N_2 U_p}{V}\left(1 + \frac{N_2 U_2}{2V}\right) - \frac{mN_2 U_2}{V}\left(1 + \frac{N_2 U_2}{2V}\right) \quad (35)$$

In eq 35, where the molecular volume of water is denoted by V°_1 and U_p is the volume excluded by the protein-polymer complex, a simple physical interpretation can be ascribed to each of the terms. The first term accounts for the loss of configurations (states) accessible to the system, due to the m polymer coils complexing with the proteins, under hypothetical conditions such that excluded-volume interactions between polymers and between the protein–polymer complex and polymers are negligible, that is, $U_2 = 0$ and $U_p = 0$, respectively. The last two terms account for the influence of these excluded-volume interactions on the free-energy term, F_5. Specifically, the second term accounts for a restriction on the configurations available to the system, as compared to the $U_p = 0$ case, due to a fraction of the system volume, U_p/V, being excluded to polymer coils by the volume of the protein–polymer complex. Clearly, this reduction in the free volume of the system increases the free energy of the polymer solution. The last term describes the increased freedom experienced by the $N_2 - m$ free polymer coils remaining in solution, which results from the removal of m polymer coils from solution to form the protein–polymer complex. That is, the complexation of the m polymer coils with the protein reduces the "cluttering" of the free polymer coils in solution.

The truncation present in eq 35 is similar to that discussed in section 5.1, and the same considerations discussed at that stage apply here with the exception of the treatment for Θ-solvent conditions. To treat Θ-solvent conditions, in addition to setting $U_2 = 0$ in eq 35 and $\nu = 0$ in eqs 32 and 34, one must necessarily include the three-body interactions between polymer segments in the system.[17] The failure to include these interactions will result in the prediction of $m = \infty$, as there will be no mechanism to oppose the adsorption of increasing numbers of polymer molecules onto the protein surface. Due to this complication, which does not arise in the treatment of Θ-solvent conditions for pictures 1 (no attraction) and 2 (weak attraction), we have not treated Θ-solvent conditions for picture 3. Rather, we have concentrated on the solvent conditions for which $U_2 > 0$, which is the relevant solvent condition for PEO in water. Furthermore, since the determination of the form of the free-energy change arising from the interactions of the protein and the polymers is not analytic and involves the summation of five terms (see below), it is important to establish the correct magnitude for the entropy term. By use of $\chi = 0.45$, corresponding to PEO in water at 25 °C,[67,68] and the Flory–Krigbaum theory[75] to estimate the magnitude of U_2, it was determined that the truncation of the expansion in terms of N_2U_2/V at quadratic order (see eqs 12 and A1) cannot be justified for polymer concentrations of 10% w/w and PEO molecular weights in the range 3000–9000 Da. Therefore, we have pursued an alternative semiempirical approach, determining U_2 within the context of the existing theoretical framework through a comparison to independent experimental vapor pressure data for aqueous PEO solutions.[76] That is, from eq 12, the chemical potential of water in an aqueous PEO solution can be derived,[49] and from this the vapor pressure depression of aqueous PEO solutions can be evaluated[76] as a function of U_2. Note that in the context of this approach, U_2 should not be strictly regarded as an excluded volume for binary interactions between polymers since it can also reflect higher order interaction terms. A comparison of the predicted vapor pressure depression of aqueous PEO solutions of approximately 10% w/w polymer with experimental measurements[76] predicts a U_2 of similar magnitude to that obtained from the Flory–Krigbaum theory.[75] Specifically, by interpolating between vapor pressure depression data for aqueous PEO solutions having number-average molecular weights of 3800 and 9000 Da, we predict that U_2 is given by the following empirical form

$$U_2 \sim 0.80a^3N^{1.6} \quad (36)$$

Note that the exponent of N in eq 36 appears physically reasonable as it falls between the limits of $^3/_2$ and $^9/_5$, expected for Θ- and athermal-solvent conditions, respectively. Although we have resorted to a semiempirical treatment of polymer–polymer interactions, importantly, through a comparison to binary PEO–water vapor pressure data we have established that our estimate of the magnitude of these interactions is accurate and will not lead to artifacts in predicted protein partitioning behavior. U_p, the excluded volume characterizing the interactions of the protein–polymer complex and free polymer coils, was estimated by eq 17, where the protein radius R_p is replaced by the radius of the protein–polymer complex $R_p + D$.

The equilibrium free energy of interaction of the protein and the polymers is obtained by minimizing the total free energy, $\delta A^\circ_{p,t,i}$, obtained by summing the contributions in eqs 32, 34, and 35, with respect to the number of polymers in the adsorbed layer, m, and the average characteristic equilibrium thickness of the adsorbed layer, D. A steepest gradient descent algorithm was used in the minimization process. Equation 8 was used to relate the change in free energy, $\delta A^\circ_{p,t,i}$, to the protein partition coefficient, $\Delta \ln K_p$. The predicted dependence of $\Delta \ln K_p$ on polymer molecular weight, protein size, and polymer segment–protein surface sticking energy was examined subject to the uncertainty in the order unity prefactors. Although variation of the numerical prefactors, k_1–k_4, yields quantitative changes in $\Delta \ln K_p$, the predicted qualitative behavior remains unchanged. For the purpose of the discussions that follow, we have assigned the order unity numerical prefactors, k_1–k_4, the numerical values of 1.

The qualitative dependence of $\Delta \ln K_p$ on the number of polymer segments per coil, N, is shown in Figure 6. For a given polymer segment–protein surface sticking energy, ϵ, an adsorbed layer of polymer will form about the protein only above a critical polymer size, denoted by N^*. A polymer smaller than the critical size will not be confined to an adsorbed layer and is free to diffuse about the bulk polymer solution. This is the scenario presented in picture

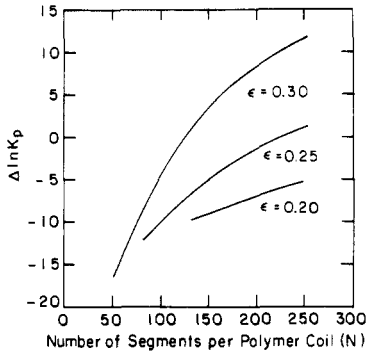

Figure 6. Predicted behavior of the protein partition coefficient for picture 3 with increasing polymer size, N, for sticking energy values $\epsilon = 0.20, 0.25$, and 0.30 and $R_p = 10a$. Note that the order unity prefactors, k_1–k_4, were assigned the numerical values of unity in Figure 6, although this should not be taken to suggest that the predictions are quantitative. For details, see section 5.3.

2; see section 5.2. The critical polymer size required to form an adsorbed layer increases with a decrease in the strength of the interaction between the polymer segments and the protein surface. For polymers larger than the critical polymer size, an increase in the polymer molecular weight, or equivalently in N, causes the protein to partition toward the polymer species. This is a result of a more favorable interaction of polymer and protein with increasing polymer molecular weight.

The qualitative behavior predicted for $\Delta \ln K_p$ in picture 3, depicted in Figure 6, is opposite to that observed in available experimental data for the partitioning of proteins shown in Figure 1 (recall that N is proportional to the polymer molecular weight). To date, the trends that we predict in Figure 6 for picture 3 have not been observed experimentally in two-phase aqueous polymer systems. Indeed, it is interesting that the above scaling arguments predict that an enhanced interaction of the polymer segments and the partitioning colloids will produce a qualitatively different behavior from that traditionally observed. For example, in phase systems with flexible polyelectrolytes, attractive electrostatic interactions of the charges residing on the polymer with those residing on the protein surface may be of sufficient strength to cause the confined adsorption of the polyelectrolyte onto the protein surface. Alternatively, the partitioning of solutes more hydrophobic than the hydrophilic proteins partitioned to date could provide a realization of the predictions of picture 3. Such solutes may include, for example, the more hydrophobic proteins or gold sols.

6. Conclusions

In this paper we have presented a new molecular thermodynamic description of the interactions of globular proteins and flexible nonionic polymers, which influence the partition of proteins in two-phase aqueous polymer systems. In particular, we have described the changing nature of the polymer solution phase from one of identifiable polymer coils to one of an entangled web or net of polymers, with increasing polymer molecular weight. For systems containing the polymer PEO, the transition in the nature of the top PEO-rich polymer solution phase is shown to be the origin of trends observed in measurements of the protein partition coefficient as a function of PEO molecular weight. In this paper, we have focused on describing the interactions of low molecular weight polymers and proteins.

In addition to the novel physical pictures proposed for the interactions of polymers and proteins in two-phase aqueous polymer systems, we have proposed descriptions for the free energy of interaction within each of the pictures and related this quantity, through a statistical thermodynamic framework, to the experimentally measured protein partition coefficient. To provide the connection between the molecular properties of the polymers and the thermodynamic parameters within the framework, we have utilized the results of scaling arguments. For our purposes, a scaling approach appears to provide a useful qualitative description of the protein partition coefficient and suggests qualitatively different trends in the protein partition coefficient with polymer molecular weight for the three scenarios investigated. Although our description of picture 2 can at best be qualitative when using the scaling relations (without known numerical prefactors) the statistical thermodynamic framework presented is suitable for the development of a more detailed description.

In this paper we have not speculated in detail on the origin of the attraction incorporated in picture 2, although we have discussed briefly the influence of the range of the attraction. In particular, when dealing with such small colloidal systems, where the role of van der Waals interactions may be important, the concept of a polymer interaction with the *surface* of the protein may not be appropriate. That is, the influence of the volumes and geometries of the interacting bodies on the interaction, as well as the possible long-range nature of the forces, may be important. Also, we have not treated in detail the potentially important role of water in protein partitioning. Such considerations may be important in proposing a more detailed statistical thermodynamic description of picture 2.

It is further evident from this approach that there is a clear need for alternative experimental studies to provide independent evidence for the existence of weak attractive interactions between this class of proteins and PEO. To this end, measurements using light scattering and neutron scattering, analogous to those performed in the anionic surfactant–polymer systems, may be illuminating.

Finally, a few comments are in order regarding the interactions of high molecular weight polymer coils and proteins. The term high molecular weight polymer refers to polymers of sufficient size to be capable of extensive interpenetration. Specifically, for typical PEO concentrations encountered in two-phase aqueous polymer solutions (10% w/w), PEO coils with molecular weights much greater than approximately 10 000 Da are extensively overlapping in solution. In section 4, we noted that in solutions of this type the identities of the individual polymer coils are lost within an entangled mesh or web of polymer. Consequently, the properties of the polymer solution should become independent of the properties of the individual polymer coils, for example, the polymer molecular weight. The observations in section 2 (see Figure 1) are consistent with this expectation, since it was stressed that the partition coefficients of proteins measured in two-phase aqueous polymer systems are insensitive to the polymer molecular weight in the limit of high polymer molecular weights.

In the limit of high polymer molecular weight, where extensive entanglements of the polymer coils are observed, the characteristic length scale of the polymer solution is no longer the polymer radius of gyration, R_g, but instead the mesh size of the polymer web or net. For the range of PEO concentrations encountered in the top PEO-rich phase in two-phase aqueous polymer systems, the mesh size is comparable to the sizes of small proteins partitioned in these systems. Significantly, the protein sizes are not always much larger or smaller than the polymer mesh size and consequently the correlations and fluctuations among the polymer segments can influence the interactions of

polymer segments with the protein. In ongoing work, we have proposed possible physical pictures for the high molecular weight polymer solution phases containing proteins, complementary scaling–thermodynamic descriptions, and experimental measurements.[77] A detailed description will be presented elsewhere.

Although many improvements of the current developments outlined in this paper are readily evident, the present work establishes a physically sound statistical thermodynamic framework on which these developments may be founded. Furthermore, the qualitative predictions of the protein partition coefficients suggest a direction for a more detailed description of the interactions influencing protein partitioning in two-phase aqueous polymer systems.

Acknowledgment. Support for this work was provided by the National Science Foundation (NSF) through the Biotechnology Process Engineering Center at MIT under Grant CDR-88-03014. N.L.A. is grateful to the George Murray Scholarship Fund of the University of Adelaide for financial support. In addition, D.B. was supported, in part, through a NSF Presidential Young Investigator Award and NSF Grant DMR-84-18718 administered by the Center for Materials Science and Engineering at MIT. D.B. is also grateful for the support by the Texaco-Mangelsdorf Career Development Professorship at MIT. Finally, the authors acknowledge very helpful discussions with Bernard Cabane of CEN-Saclay, France, at the outset of this work.

Appendix

The derivation of the entropy of mixing term, F_5, presented in section 5.3 starts with eq 12 and a modified form of eq 13, where the latter is altered to account for the reduction in the number of free polymer coils in the system from N_2 to $N_2 - m$. In addition, substituting $N_p = 1$ on the right-hand side of eq 13 yields

$$\ln \Omega_{N_p=1} = \ln (A_2^{N_2-m} A_p) - \ln ((N_2 - m)!) + (N_2 - m) \ln (V - U_p) + \ln V - \frac{U_2(N_2 - m)^2}{2(V - U_p)} - \frac{U_2^2(N_2 - m)^3}{6(V - U_p)^2} \quad \text{(A1)}$$

where U_p is the volume excluded by the protein–polymer complex (that is, the protein and m adsorbed polymer coils) to the polymer coils. Subtracting eq 12 from eq A1 leads to the translational entropy change accompanying the mixing of the protein–polymer complex and the remaining $N_2 - m$ polymers, ΔS_{mix}, where

$$\frac{\Delta S_{mix}}{k} = -m \ln (A_2 V) + \ln (A_p V) - N_2 \ln \left(1 - \frac{m}{N_2}\right) + m \ln (N_2 - m) - m + (N_2 - m) \ln \left(1 - \frac{U_p}{V}\right) + \frac{U_2 N_2^2}{2V} - \frac{U_2(N_2 - m)^2}{2V\left(1 - \frac{U_p}{V}\right)} + \frac{U_2^2 N_2^3}{6V^2} - \frac{U_2^2(N_2 - m)^3}{6V^2\left(1 - \frac{U_p}{V}\right)^2} \quad \text{(A2)}$$

Expanding eq A2 to leading order in the expansion parameters, U_p/V ($\ll 1$) and m/N_2 ($\ll 1$), yields

$$\frac{\Delta S_{mix}}{k} = -m \ln \left(\frac{A_2 V}{N_2}\right) + \ln (A_p V) - \frac{N_2 U_p}{V}\left(1 + \frac{N_2 U_2}{2V}\right) + \frac{m N_2 U_2}{V}\left(1 + \frac{N_2 U_2}{2V}\right) \quad \text{(A3)}$$

In eq A3, the term $\ln (A_p V)$ represents the entropy of mixing a single protein in a volume V in the absence of free polymers. As the quantity of interest is the deviation in the entropy of mixing from that in the absence of polymer–protein excluded-volume interactions, this term is subtracted from eq A3 (see also section 5.1).

In order to evaluate the entropy of mixing from eq A3, the value of A_2 must be determined. Recall that A_2 is defined as follows: if $V - U_t$ is the free volume accessible to a polymer coil upon placement in the system, where U_t is the total system volume that is excluded by the other molecules in the system, then $A_2(V - U_t)$ is the number of ways to place the center of mass of the polymer coil in the available system volume, $V - U_t$. We have defined A_2 as

$$A_2 = 1/V_1^\circ \quad \text{(A4)}$$

where V_1° is the molecular volume of the solvent. That is, we assumed that the volume of a solvent molecule defines an imaginary lattice of cells, each of which can accommodate the center of mass of a polymer coil. Note that A_2 is independent of the polymer coil size and that the influence of the polymer coil size on the configurations available to the system is reflected through the free volume available to the polymer coil. Using eq A4 in eq A3, subtracting $\ln (A_p V)$ from eq A3 (as discussed above), and recognizing that $F_5 = -\Delta S_{mix}^{ex}/k$ lead to eq 35 in section 5.3.

Nomenclature

a	polymer segment size
A_c	area of contact between polymer coil and protein
A_2, A_p	proportionality constants for excluded volumes of polymer coils and proteins, respectively.
b	sphere radius
c	weight fraction of polymer
c^*	weight fraction of polymer at entanglement
$c_{p,i}$	protein concentration in phase i
D	thickness of adsorbed polymer layer
f	fraction of polymer segments in adsorbed polymer layer at protein surface
F_i	ith contribution to the protein chemical potential
F_{att}	attractive contribution to protein chemical potential
k	Boltzmann factor
K_p^{att}	attractive contribution to the protein partition coefficient
K_p	protein partition coefficient
k_i	order unity prefactor
m	number of polymer coils in the adsorbed polymer layer
$\langle m_s \rangle$	average number of polymer segment contacts between polymer coil and protein
M	molecular weight
N	number of polymer segments per coil
N_2	number of polymer coils
N_p	number of protein molecules
p	order unity numerical prefactor
R_{eff}	radius characterizing area of contact between polymer and protein
R_p	protein radius
R_g	polymer coil radius of gyration
S_p	surface area of protein
T	temperature
U_p	volume excluded by a protein molecule to a polymer coil
U_j	volume excluded by the $j - 1$ polymer coils
V	system volume

V_1°	molecular volume of solvent
V_c	volume described by the polymer coil center of mass during attractive interactions with the protein
$z_{p,i}$	net protein charge in phase i
α, β, γ	numerical exponents
$\gamma_{p,i}$	protein activity coefficient in phase i
$\Delta\psi$	electrical potential difference
$\delta A^\circ_{p,t,i}$	Helmoltz free energy change with the introduction of a protein into the top phase at conditions i
$\delta S^\circ_{p,t,i}$	entropy change (see above)
ϵ	sticking free energy of a polymer segment at the protein surface
$\mu_{p,i}$	protein chemical potential in phase i
$\mu^\circ_{p,i}$	protein chemical potential in the standard state
$\mu^\circ_{p,i,j}$	protein chemical potential in the standard state in phase i at condition j
ν	binary polymer–solvent interaction parameter
ρ^*	characteristic density of polymer segments within a coil
ϕ	volume fraction of polymer
ϕ_t, ϕ_s	volume fraction of polymer in top phase and at protein surface, respectively
χ	Flory–Huggins polymer–solvent interaction parameter
ψ_i, ψ_0	electrical potentials in phase i and the reference phase, respectively
$\Omega_{N_p=1}$, $\Omega_{N_p=0}$	number of configurations of the polymer solution with and without protein, respectively

References and Notes

(1) Tokiwa, F.; Tsujii, K. *Bull. Chem. Soc. Jpn.* **1973**, *46*, 2684.
(2) Shirahama, K. *Colloid Polym. Sci.* **1974**, *252*, 978.
(3) Shirahama, K.; Ide, N. *J. Colloid Interface Sci.* **1976**, *54*, 450.
(4) Cabane, B. *J. Phys. Chem.* **1977**, *81*, 1639.
(5) Cabane, B.; Duplessix, R. *J. Phys.* **1982**, *43*, 1529.
(6) Cabane, B.; Duplessix, R. *J. Phys.* **1987**, *48*, 651.
(7) Goddard, E. D. *Colloids Surf.* **1986**, *19*, 255.
(8) Goddard, E. D. *Colloids Surf.* **1986**, *19*, 301.
(9) Heller, W.; Pugh, T. L. *J. Chem. Phys.* **1956**, *22*, 1778.
(10) Woodhead, J. L. *J. Phys., Colloq. C1* **1986**, *47*, C1-3.
(11) Napper, D. H. *Polymeric Stabilization of Colloidal Dispersions*; Academic Press: London, 1983.
(12) Gekko, K.; Timasheff, S. N. *Biochemistry* **1981**, *20*, 4667.
(13) Ingham, K. C. *Arch. Biochem. Biophys.* **1977**, *184*, 59.
(14) Ingham, K. C. *Arch. Biochem. Biophys.* **1978**, *186*, 106.
(15) Middaugh, C. R.; Lawson, E. Q. *Anal. Biochem.* **1980**, *105*, 364.
(16) Alexander, S. *J. Phys.* **1977**, *38*, 977.
(17) Pincus, P. A.; Sandroff, C. J.; Witten, T. A. *J. Phys.* **1984**, *45*, 725.
(18) Marques, C. M.; Joanny, J. F. *J. Phys.* **1988**, *49*, 1103.
(19) Albertsson, P. A. *Partition of Cell Particles and Macromolecules*; Wiley: New York, 1986.
(20) Walter, H., Brooks, D. E., Fisher, D., Eds. *Partitioning in Aqueous Two-Phase systems*; Academic Press: New York, 1985.
(21) Kula, M. R.; Kroner, K. H.; Hustedt, H. *Adv. Biochem. Eng.* **1982**, *24*, 73.
(22) Abbott, N. L.; Hatton, T. A. *Chem. Eng. Progr.* **1988**, *84* (8), 31.
(23) Sasakawa, S.; Walter, H. *Biochemistry* **1972**, *14*, 2760.
(24) Albertsson, P.-A.; Cajarville, A.; Brooks, D. E.; Tjerneld, F. *Biochim. Biophys. Acta* **1987**, *926*, 87.
(25) Albertsson, P.-A. *Adv. Protein Chem.* **1974**, *24*, 309.
(26) Hustedt, H.; Kroner, K. H.; Stach, W.; Kula, M.-R. *Biotechnol. Bioeng.* **1978**, *20*, 1989.
(27) Baskir, J. N.; Hatton, T. A.; Suter, U. W. *J. Phys. Chem.* **1989**, *93*, 2111.
(28) Diamond, A. D.; Hsu, J. T. *Biotechnol. Bioeng.* **1989**, *34*, 1000.
(29) King, R. S.; Blanch, H. W.; Prauznitz, J. M. *AIChE J.* **1988**, *34*, 1585.
(30) Shanbhag, V. P.; Axelsson, C. G. *Eur. J. Biochem.* **1975**, *60*, 17.
(31) Shanbhag, V. P.; Johansson, G. *Eur. J. Biochem.* **1979**, *363*, 1979.
(32) Johansson, G.; Hartman, A.; Albertsson, P.-A. *Eur. J. Biochem.* **1973**, *33*, 379.
(33) Johansson, G.; Andersson, M. *J. Chromatogr.* **1984**, *303*, 39.
(34) Joelsson, M.; Johansson, G. *Enzyme Microb. Technol.* **1987**, *99*, 233.
(35) Joelsson, M.; Johansson, G. *Appl. Biochem. Biotechnol.* **1986**, *13*, 15.
(36) Johansson, G. *Mol. Cell Biochem.* **1974**, *4*, 169.
(37) Johansson, G. *Biochim. Biophys. Acta* **1970**, *221*, 387.
(38) Bamberger, S.; Seaman, G. V. F.; Brown, J. A.; Brooks, D. E. *J. Colloid Interface Sci.* **1984**, *99*, 187.
(39) Abbott, N. L.; Blankschtein, D.; Hatton, T. A. *Bioseparation* **1990**, *1*, 191.
(40) Baskir, J. N.; Hatton, T. A.; Suter, U. W. *Biotechnol. Bioeng.* **1989**, *34*, 541.
(41) Brooks, D. E.; Sharp, K. A.; Fisher, D. In *Partitioning in Aqueous Two-Phase Systems*, Walter, H., Brooks, D. E., Fisher, D. Eds.; Academic Press: New York, 1985; Chapter 2.
(42) Flory, P. J. *Principles of Polymer Chemistry*; Cornell University Press: Ithaca and London, 1986.
(43) Huggins, M. L. *J. Phys. Chem.* **1941**, *9*, 440.
(44) Baskir, J. N.; Hatton, T. A.; Suter, U. W. *Macromolecules* **1987**, *20*, 1300.
(45) Scheutjens, J. M. H. M.; Fleer, G. J. *J. Phys. Chem.* **1979**, *83*, 1619.
(46) Scheutjens, J. M. H. M.; Fleer, G. J. *J. Phys. Chem.* **1980**, *84*, 179.
(47) Forciniti, D.; Hall, C. K. *ACS Symp. Ser.* **1990**, *419*, 53.
(48) de Gennes, P.-G. *Scaling Concepts in Polymer Physics*; Cornell University Press: Ithaca, NY, and London, 1988.
(49) Tanford, C. *Physical Chemistry of Macromolecules*; Wiley: New York, 1961.
(50) Baskir, J. N. Ph.D. Thesis, Massachusetts Institute of Technology, 1988.
(51) Abbott, N. L.; Blankschtein, D.; Hatton, T. A., to be published in *Macromolecules*.
(52) Tadokoro, H.; Chatani, Y.; Yoshihara, T.; Tahara, S.; Murahashi, S. *Makromol. Chem.* **1964**, *73*, 109.
(53) Koenig, J. L.; Angood, A. C. *J. Polym. Sci., A-2* **1970**, *8*, 1787.
(54) Maxfield, J.; Shepherd, I. W. *Polymer* **1975**, *16*, 505.
(55) Liu, K.-J.; Parsons, J. L. *Macromolecules* **1969**, *2*, 529.
(56) Liu, K.-J.; Anderson, J. E. *Macromolecules* **1970**, *3*, 163.
(57) Hammes, G.; Roberts, P. B. *J. Am. Chem. Soc.* **1968**, *90*, 7119.
(58) Bailey, F. E.; Kucera, J. L.; Imhof, L. G. *J. Polym. Sci.* **1958**, *32*, 517.
(59) Beech, D. R.; Booth, C. *J. Polym. Sci., A-2* **1969**, *7*, 575.
(60) Molyneux, P. *Water Soluble Synthetic Polymers; Properties and Behavior 1*; CRC Press: Boca Raton, FL, 1982.
(61) Bailey, F. E.; Koleske, J. V. *Poly(ethyleneoxide)*; Academic Press: New York, 1976.
(62) Ingham, K. *Arch. Biochem. Biophys.* **1977**, *184*, 59.
(63) Jones, M. N. *J. Colloid Interface Sci.* **1967**, *23*, 36.
(64) Nagarajan, R.; Kalpacki, B. In *Microdomains in Polymer Solutions*; Dubin, P., Ed.; Plenum Press: New York, 1982.
(65) Modell, M.; Reid, R. C. *Thermodynamics and its Applications*, 2nd ed.; Prentice-Hall: London, 1983.
(66) Ruckenstein, E.; Chi, J. C. *J. Chem. Soc., Faraday Trans 2* **1975**, *71*, 1690.
(67) Edmond, E.; Ogston, A. G. *Biochem. J.* **1968**, *109*, 569.
(68) Rogers, J. A.; Tam, T. *Can. J. Pharm. Sci.* **1977**, *12*, 65.
(69) Hermans, J. *J. Chem. Phys.* **1982**, *77*, 2193.
(70) Hermans, J. J.; Hermans, J. *J. Polym. Sci.* **1984**, *22*, 279.
(71) Jansons, K. M.; Phillips, C. G. *J. Colloid Interface Sci.* **1990**, *137*, 75.
(72) Abbott, N. L.; Blankschtein, D.; Hatton, T. A., to be published in *Macromolecules*. U_p was evaluated by reptation to generate the configurations of a self-avoiding polymer chain on a cubic lattice in the vicinity of an impenetrable sphere.
(73) Abbott, N. L.; Blankschtein, D.; Hatton, T. A. to be published in *Macromolecules*. $\langle m_s \rangle$ was evaluated, by the method described in ref 72, as the number of polymer segments within a distance a from an impenetrable sphere surface, averaged over configurations that do not penetrate the sphere volume.
(74) Lee, S. H.; Ruckenstein, E. *J. Colloid Interface Sci.* **1988**, *125*, 365.
(75) Flory, P. J.; Krigbaum, W. R. *J. Chem. Phys.* **1950**, *18*, 1086.
(76) Haynes, C. A.; Beynon, R. A.; King, R. S.; Blanch, H. W.; Prausnitz, J. *J. Phys. Chem.* **1989**, *93*, 5612.
(77) Abbott, N. L.; Blankschtein, D.; Hatton, T. A. 6th International Conference on Partitioning in Aqueous Two-Phase Systems, Assmannshausen, West Germany, 1989.